Static Model Using Crossing-Symmetric Off-Shell Equations Satisfying Two-Particle Unitarity*

DAVID F. FREEMAN, GERALD R. NORTH,† AND MORTON H. RUBIN
Department of Physics, University of Pennsylvania, Philadelphia, Pennsylvania 19104
(Received 18 August 1969)

Off-shell equations for the π^-p and π^+p elastic scattering amplitudes are derived for a static model, based on charged scalar theory. These amplitudes satisfy elastic unitarity below the three-particle cut and are related by crossing symmetry. The equations are solved numerically in the bound-state region for the entire range of coupling, and the results compared with the known results of charged scalar theory. In particular, calculations of the bound-state N^{++} are reasonable. Possible extensions to more realistic models are discussed.

I. INTRODUCTION

RECENTLY, a number of people have been interested in studying crossing-symmetric off-shell equations. This interest stems in part from attempts to find bootstrap solutions in quantum field theory[1] and in part from the ancient desire to find any way of making dynamical calculations.[2] In this paper our motivation is the latter of these two reasons. It is hoped that by solving a set of equations for off-shell two-particle scattering amplitudes which incorporate elastic unitarity and crossing symmetry, we can obtain a reasonable first approximation to the exact scattering amplitudes for a field theory.

Our starting point is the venerable charged scalar static model.[3] As always, this model is chosen because it is the simplest nontrivial model available. In addition, there is an extensive literature dealing with various approximate solutions to this model which provide us a basis for comparison with our numerical results. Our procedure, carried out in Sec. II, is to derive a pair of Lippmann-Schwinger equations describing π^-p and π^+p elastic scattering. The solutions of these equations are required to satisfy elastic unitarity below the lowest production threshold and to be related to each other through off-shell crossing symmetry.

The general properties of these solutions are well known. We review them in Sec. III, paying particular attention to the specific properties engendered by the approximations required to set up our equations.

The aim of this work is to obtain detailed numerical solutions to the equations derived in Sec. II. In order to make headway, we restricted ourselves to studying our equations in the bound-state region of the energy variable. The numerical procedure is discussed in Sec. IV.

In Sec. V, we display and analyze our results.

II. MODEL

The model we work with is defined in terms of Lippmann-Schwinger equations for the scattering amplitudes $T_{\omega\omega'}(E)$ describing π^-p elastic scattering and $T^{\times}{}_{\omega\omega'}(E)$ describing π^+p elastic scattering. ω (ω') is the energy of the outgoing (incoming) pion and E is the total energy of the system. The on-shell amplitude is $T(\omega)=T_{\omega\omega}(\omega)$. T and $T^{\times}$ are to be related through the off-shell crossing relation

$$T_{\omega\omega'}(E)=T^{\times}{}_{-\omega'-\omega}(E-\omega-\omega'). \tag{2.1}$$

In addition to Eq. (2.1), T and $T^{\times}$ must separately satisfy two-particle unitarity below the three-particle threshold.

The equations for T and $T^{\times}$ are derived as follows.[4,5] T is first written as a sum of three terms,

$$T(E)=V(E)+L(E)+R(E), \tag{2.2}$$

where $V(E)$ is a potential term which is assumed to be known, $L(E)$ has no pole terms or two-particle cuts, and $R(E)$ has the two-particle unitary cut. An equation for $R(E)$ may be derived by formally considering any diagram that can contribute to it. Starting from the left of any such diagram, proceed toward the right until you reach the first two-particle intermediate state. To the left of this intermediate state only V or L can occur, while to the right the full T matrix can occur. Thus,

$$R(E)=[V(E)+L(E)]G(E)T(E), \tag{2.3}$$

where $G(E)=(E-H_0)^{-1}$ is the free Green's function. Combining (2.1) and (2.3) gives the Lippmann-Schwinger equation for T, with $V+L$ serving as an effective potential. In the language of the Bethe-Salpeter equation, $L+V$ corresponds to the irreducible kernel for T. $T^{\times}$ is treated in exactly the same manner as

* Supported in part by the Atomic Energy Commission and by the National Science Foundation, under Contract No. NSF-GP-8414.

† Present address: University of Missouri, St. Louis, 8001 Natural Bridge Road, St. Louis, Mo. 63121.

[1] See J. G. Taylor's article in *Lectures in Theoretical Physics* (Gordon and Breach, Science Publishers, Inc., New York, 1968), Vol. X-4.

[2] R. Blankenbecler, in *Proceedings of the International Conference on Particles and Fields, Rochester, 1967* (Wiley-Interscience, Inc., New York, 1967).

[3] G. Wentzel, *Quantum Theory of Fields* (Wiley-Interscience, Inc, New York, 1949), p. 53.

[4] I. T. Diatlov and K. A. Ter-Martirosian, Zh. Eksperim. i Teor. Fiz. 30, 416 (1956) [English transl.: Soviet Phys.—JETP 3, 454 (1956)]; also see R. W. Haymaker and R. Blankenbecler, Phys. Rev. 171, 1581 (1968).

[5] Our normalization is specified in Appendix A.

T, i.e.,

$$T^{\times}(E)=V^{\times}(E)+L^{\times}(E)+R^{\times}(E) \tag{2.4}$$

and

$$R^{\times}(E)=[V^{\times}(E)+L^{\times}(E)]G(E)T^{\times}(E). \tag{2.5}$$

In order to satisfy Eq. (2.1), it is required that

$$\begin{aligned} V^{\times}{}_{\omega\omega'}(E)&=V_{-\omega'-\omega}(E-\omega-\omega'),\\ L^{\times}{}_{\omega\omega'}(E)&=R_{-\omega'-\omega}(E-\omega-\omega'),\\ L_{\omega\omega'}(E)&=R^{\times}{}_{-\omega'-\omega}(E-\omega-\omega'). \end{aligned} \tag{2.6}$$

The last two equations are consistent with our requirements on the singularity structure of L, $L^{\times}$, R, and $R^{\times}$. This is easily seen by studying perturbation-theory diagrams. The general result follows upon noting that the unitarity cut in E of $R(R^{\times})$ goes over to a left-hand "potential" cut in $L^{\times}(L)$ for ω, $\omega'\geq 1$. On the energy shell $L^{\times}{}_{\omega\omega}(\omega+i\epsilon)=R_{-\omega-\omega}(-\omega-i\epsilon)$ and $L_{\omega\omega}(\omega+i\epsilon)=R^{\times}{}_{-\omega-\omega}(-\omega-i\epsilon)$ as usual.

To complete the model it is only necessary to specify V. In this work we take V to be the neutron-pole term,

$$V_{\omega'\omega}(E)=f(k')\frac{g_0{}^2}{E-m_0}f(k), \tag{2.7}$$

where g_0 is the unrenormalized pion-nucleon coupling constant, m_0 is the unrenormalized neutron mass, and $f(k)$ is a form factor (which is an even function of ω). The relation of this notation to the charged scalar static-model Hamiltonian is given in Appendix A.

Equations (2.3)–(2.7) provide coupled nonlinear integral equations which we have solved numerically for the choice of f given by[5]

$$f^2(k)=2\pi^2/(\alpha^2k^2+1),$$

where α^{-1} is a cutoff momentum. The limit $\alpha\to 0$ corresponds to a point nucleon.

III. PROPERTIES OF MODEL

A. Perturbative Solution

Starting with V and $V^{\times}$, we can generate a perturbation series for T and $T^{\times}$. The lowest orders of this series are shown in Fig. 1. Elastic unitarity is satisfied up to sixth order, while three-particle unitarity is not. To achieve the latter, it would be necessary to add Figs. 2(a) and 2(b) to $R^{\times}$ and Fig. 2(c) to $R^{\times}$. These three diagrams and their crossing-related partners are the lowest-order ones omitted in the present model. While including these diagrams would not violate crossing symmetry and two-particle unitarity, neither are they necessary to satisfy these conditions. It is in this sense that the model of Sec. II is the "simplest" of those possible under the given restrictions.

Figure 2(a) is absent simply because it is never generated by two-particle unitarity. Figures 2(b) and 2(c) differ from diagrams that do appear in the perturbation series by the appearance of a bubble on the proton line. In fact, in contrast to the neutron, proton modifications are never generated. This is one important aspect of the model being "simplest." The consequence of this unsymmetric treatment of nucleons is discussed below.

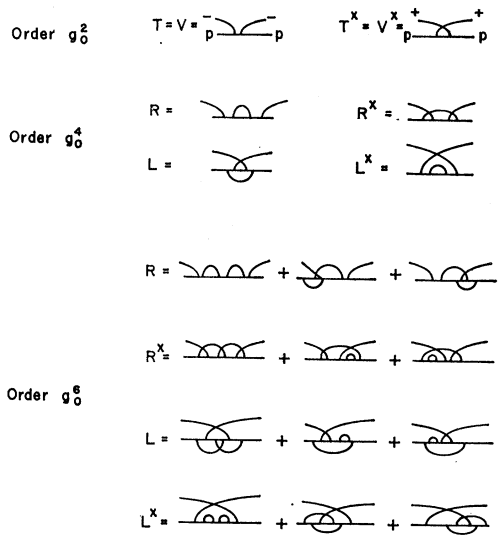

FIG. 1. Lowest-order perturbation diagrams for π^-p and π^+p elastic scattering.

It is clear from Fig. 1 that each order of perturbation theory adds inelastic states with more and more mesons. These states increase the attraction of the effective potential; since multiparticle unitarity is not imposed, this attraction may grow inordinately large. In particular, it could produce some inelastic bound states known to be absent in charged scalar theory,[6,7] but occurring in related models.[8]

B. General Features

L and $L^{\times}$ are both real symmetric operators below the three-particle cut. This is suggested by perturbation theory (see Fig. 1) and can be proved from the equations of Sec. III. Consequently T and $T^{\times}$ satisfy elastic unitarity below the three-particle cut, as is desired.

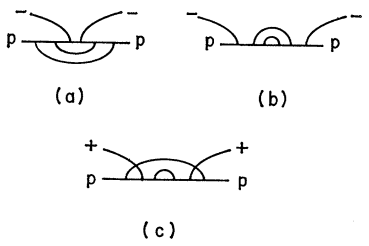

FIG. 2. Lowest-order perturbation diagrams omitted from model.

[6] A. Pais and R. Serber, Phys. Rev. **105**, 1636 (1957). This paper contains references to earlier work.
[7] C. J. Goebel, Phys. Rev. **109**, 1846 (1958).
[8] J. B. Bronzan, Phys. Rev. **154**, 1545 (1967).

It is useful to consider the formal solution to the equation for T assuming L is known. Equations (2.2) and (2.3) then yield a two-potential Lippmann-Schwinger equation with one of the potentials being separable. The solution to this type of equation is well known, and is only briefly reviewed here. T has the general form

$$T(E)=\mathfrak{L}(E)+g_0^2\Gamma(E)G_N(E)\Gamma(E)^\dagger, \tag{3.1}$$

$$\mathfrak{L}(E)=[1-L(E)G(E)]^{-1}L(E), \tag{3.2}$$

$$G_N^{-1}(E)=E-m_0-\Delta(E) -g_0^2\langle f|G(E)\mathfrak{L}(E)G(E)|f\rangle, \tag{3.3}$$

$$\Delta(E)=g_0^2\langle f|G(E)|f\rangle=g_0^2\int_1^\infty \frac{d\omega}{(2\pi)^2}\frac{kf^2(k)}{E-\omega}, \quad k=(\omega^2-1)^{1/2} \tag{3.4}$$

$$\Gamma(E)=[1-\mathfrak{L}(E)G(E)]|f\rangle. \tag{3.5}$$

$\mathfrak{L}(E)$ is sometimes referred to as the "potential scattering term." $G_N(E)$ is the modified neutron propagator, while $\Delta(E)$ represents the modification due to bubbles. Finally, $\Gamma(E)$ is the modified form factor. m_0 is fixed by requiring $G_N^{-1}(0)=0$, which makes the renormalized neutron mass equal to the proton mass. It may happen that G_N^{-1} has zeros other than that at $E=0$. It is known that the charged scalar model does not have a neutral isobar[6]; therefore, such extra zeros in G_N^{-1} would indicate that we had mutilated the original theory too badly. Note that poles of $\mathfrak{L}$ do not appear in T,[9] and hence cause no such difficulties.

Proton lines could be modified by replacing the propagator $G(E)=(E-H_0)^{-1}$ by Dyson's expression $Z_2^{-1}[E-H_0+\Sigma(E-H_0)]^{-1}$, where $\Sigma(z)$ is zero at $z=0$ and is analytic in the z plane cut from 1 to ∞. This form ensures that the only changes occur above the three-particle cut, since G occurs only between states of one proton and one or more mesons.

From the general theory of the Lippmann-Schwinger equation, we know that $T^\times$ has the same structure as T. For sufficiently small g_0^2 there is no bound state and the perturbation series for $T^\times$ converges. As g_0^2 increases, a bound state, the N^{++} isobar, develops just below the elastic threshold and moves along the real E axis toward the origin. The trajectory of this pole in $T^\times$ is of some interest, since its behavior is understood in strong-coupling theory.[7] Again it is possible to develop too many poles in this channel.

C. Comparison with Charged Scalar Theory

When the isobar N^{++} appears as a bound state of π^+p for sufficiently large coupling, it opens up the possibility of charge-exchange scattering, $\pi^-p\to\pi^+N^-$, where N^- is the charge-symmetry partner of N^{++}. Therefore, there should be an inelastic two-particle cut in π^-p elastic scattering resulting from the π^+N^- intermediate state. In charged scalar theory this cut emerges from the three-particle cut at the value of the coupling constant for which N^{++} just becomes bound. In the strong-coupling limit this cut exactly covers the elastic cut, and the elastic and charge-exchange cross sections become equal.

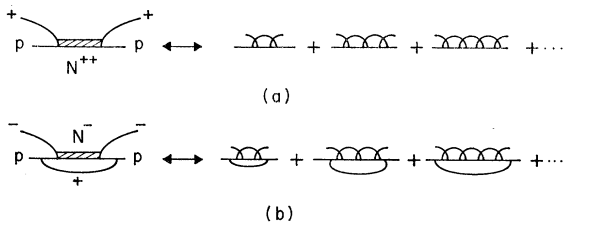

FIG. 3. (a) Diagrams contributing to the N^{++} isobar intermediate state. (b) Diagrams contributing to the inelastic two-particle intermediate state.

As pointed out above, however, in our model the scattering matrix always satisfies elastic unitarity below the three-particle cut and charge-exchange scattering, therefore, does not take place. The source of this difference between the model of Sec. II and charged scalar theory can be traced to the omission in R of diagrams without two-particle cuts. In Fig. 3 this is illustrated. Figure 3(a) shows the N^{++} and a few of the diagrams which contribute to it. Figure 3(b) shows that the related diagrams only appear in π^-p elastic scattering as terms with no two-particle cuts.

This omission means that our model must certainly disagree with charged scalar theory in the energy region of charge-exchange scattering. A difficult question is whether the omission of such charge-exchange effects is consistent with the calculation of the isobar in the bound-state region. The only way for this to be consistent is for the inelastic states above the three-particle threshold to compensate for the binding effect of the (omitted) charge-exchange intermediate state. In our model these inelastic states do contribute large binding effects.

The above objection is valid for any model with only elastic unitarity. A second departure of the model from charged scalar theory stems from the more technical feature of treating protons and neutrons asymmetrically. The renormalized propagators and vertex functions are defined by

$$G_\alpha(E)=Z_2{}^\alpha G_\alpha{}^r(E), \quad \alpha=n,p$$

$$\Gamma(E,\omega)=\langle\omega|\Gamma(E)=Z_1^{-1}\Gamma^r(E,\omega),$$

$$\lim_{E\to0}EG_\alpha{}^r(E)=1, \quad \Gamma^r(0,1)=1.$$

The coupling-constant renormalization is $g/g_0=(Z_2{}^nZ_2{}^p)^{1/2}Z_1^{-1}$, where g is the renormalized coupling constant. In charged scalar theory $Z_2{}^n=Z_2{}^p=Z_2$, so

[9] C. J. Goebel and B. Sakita, Phys. Rev. Letters **11**, 293 (1963); Y. S. Jin and S. W. MacDowell, Phys. Rev. **137**, B688 (1964).

$g/g_0=Z_2Z_1^{-1}$. In our model $Z_2^p=1$, so $g/g_0=(Z_2^n)^{1/2}Z_1^{-1}$. This means that the renormalized coupling constant may well be quite different in charged scalar theory and in our model.

IV. NUMERICAL METHODS

A. Iterative Scheme

In order to solve the system (2.3)–(2.7), it is convenient to let $R_{\omega'\omega}(E)=g_0^2f(k')r_{\omega'\omega}(E)f(k)$, $L_{\omega'\omega}(E)=g_0^2f(k')l_{\omega'\omega}(E)f(k)$, etc. Then (2.3) becomes

$$r_{\omega'\omega}(E)=\int_1^\infty d\nu[v(E)+l(E)]_{\omega'\nu}\frac{\rho(\nu)}{E-\nu}t_{\nu\omega}(E),$$
$$\rho(\nu)=g_0^2\frac{kf^2(k)}{(2\pi)^2}=\tfrac{1}{2}g_0^2\frac{k}{\alpha^2k^2+1}. \tag{4.1}$$

Next, integrals are replaced by Gaussian sums, so that Eq. (4.1) becomes

$$r_{\omega'\omega}(E)=\sum_\nu[v(E)+l(E)]_{\omega'\nu}\frac{W_\nu}{E-\nu}t_{\nu\omega}(E), \tag{4.2}$$

where the ν's are the coordinates associated with the Gaussian quadrature and W_ν is the product of the associated Gaussian weight and $\rho(\nu)$.

If $v(E)$ and $l(E)$ are known, Eq. (4.1) is a Fredholm integral equation (for $E<1$, i.e., below elastic threshold). Equation (2.2) now gives

$$r_{\omega'\omega}(E)=\int_1^\infty d\nu[v(E)+l(E)]_{\omega'\nu}\frac{\rho(\nu)}{E-\nu}[v(E)+l(E)]_{\nu\omega}+\int_1^\infty d\nu[v(E)+l(E)]_{\omega'\nu}\frac{\rho(\nu)}{E-\nu}r_{\nu\omega}(E). \tag{4.3}$$

The approximate form (4.2) is solved by matrix inversion to give

$$r_{\omega'\omega}(E)=\sum_{\alpha,\beta}[v(E)+l(E)]_{\omega'\alpha}S_{\alpha\beta}(E)\times[v(E)+l(E)]_{\beta\omega},$$
$$S_{\alpha\beta}(E)=\sum_\gamma\{1-G(E)[v(E)+l(E)]\}^{-1}_{\alpha\gamma}G_{\gamma\beta}(E), \tag{4.4}$$
$$G_{\alpha\beta}(E)=\delta_{\alpha\beta}W_\beta/(E-\beta).$$

$r^\times(E)$ has a similar solution in terms of $v^\times(E)$ and $l^\times(E)$.

Equation (4.4) and crossing symmetry suggest an iterative procedure for solving the system. Starting with a known v—which fixes the model—and an approximate l, Eq. (4.4) generates an approximate r. This r specifies $l^\times$ through crossing, which is then used in the analog of Eq. (4.4) to obtain $r^\times$. Crossing $r^\times$ then gives a new approximation for l. The crucial question is whether this iterative scheme converges.

If the iterative procedure outlined above is used with Eq. (4.3), the perturbation series for t and $t^\times$ is generated. While Eq. (4.4) is simply an algebraic rearrangement of Eq. (4.3), it is known that algebraic manipulation of nonlinear equations can markedly improve the convergence of the resulting iterative procedure.[10] In fact, with certain technical modifications described below, the iterative procedure based on Eq. (4.4) converges in the presence of weakly bound states, where the perturbation series diverges. In terms of diagrams, this procedure corresponds to regrouping the perturbation series by summing over infinite subsets of diagrams related by unitarity. For example, the first step in this iterative procedure gives r as the sum of bubbles (the chain approximation).

When the coupling constant is increased significantly beyond the value needed to form the N^{++} isobar, other more powerful methods are needed to obtain a convergent iterative procedure. These methods, which are described in Appendix B, lack any simple diagrammatic interpretation. Their justification is solely in terms of improved convergence.

B. Complications due to Crossing

Crossing as given by Eq. (2.6) is most easily put into the system by eliminating r and $r^\times$. We write

$$l^\times_{\omega'\omega}(E)=\sum_{\alpha,\beta}[v(E-\omega-\omega')+l(E-\omega-\omega')]_{-\omega\alpha}\times S_{\alpha\beta}(E-\omega-\omega')[v(E-\omega-\omega')+l(E-\omega-\omega')]_{\beta-\omega'},\quad \omega,\omega'\geq 1 \tag{4.5}$$

and its charge-symmetric partner.

From Eq. (4.5), we see that we need to calculate $l_{-\omega\alpha}(E)$, ω, $\alpha>1$; since $L(E)$ is a symmetric operator (time-reversal invariance), $l_{\omega'\omega}(E)=l_{\omega\omega'}(E)$, and we do not need an additional $l_{\beta-\omega}(E)$. Also,

$$l^\times_{-\omega'\omega}(E)=\sum_{\alpha,\beta}[v(E+\omega'-\omega)+l(E+\omega'-\omega)]_{-\omega\alpha}\times S_{\alpha\beta}(E+\omega'-\omega)[v(E+\omega'-\omega)+l(E+\omega'-\omega)]_{\beta\omega'},\quad \omega,\omega'\geq 1. \tag{4.6}$$

In our iterative scheme these matrices are found to be less convergent than those of (4.5); however, physical quantities are calculated directly from the latter, and hence this is not a serious problem.

From (4.5) and (4.6) we can see a special property of the model and indeed of off-shell charged scalar theory: The calculation can be done entirely in the region $E\leq E_0$ for E_0 fixed but arbitrary. In (4.5), if $E\leq E_0$, the energy of the right-hand side is also in the region. For (4.6) this is not true; however, the right-hand side is in the region if $E\leq E_0-\omega'$, and from (4.5) we see that this

[10] B. Noble, in *Nonlinear Integral Equations*, edited by P. M. Anselone (University of Wisconsin Press, Madison, Wisc., 1964).

is where $l_{-\omega'\omega}$ is needed to calculate $l^{\times}_{\omega'\omega}(E)$. We therefore can work entirely below any given energy E_0; we naturally take this to be the elastic threshold, $E_0=1$.

One word of caution is necessary: It is important never to exceed E_0 in the calculation; the formal property that only energies below E_0 are necessary is not of itself sufficient. For example, one might for convenience use matrices above E_0 in intermediate steps and assign arbitrary values (say, zero) to them, knowing that in an exact solution these matrices cannot contribute below E_0. This leads to severe numerical instabilities.

C. Unrenormalized Neutron Mass

For a given $V(E)$, our computational scheme now generates $L(E)$ and $L^{\times}(E)$. There remains one further point, namely, ensuring that the neutron propagator has its pole at the correct energy. As discussed in Sec. III, this is done setting $G_N^{-1}(0)=0$, fixing m_0. From Eq. (3.3), m_0 is a function of $L(E)$, which depends on the input $V(E)$; finally, m_0 is a parameter of $V(E)$, as in (2.7). This yields a consistency condition which determines m_0.

The most direct way of incorporating this condition into the iterative scheme is to use $L(E)$ at the end of each iteration to calculate an approximate m_0, and to use this mass in $V(E)$ and $V^{\times}(E)$ for the next iteration. Clearly, if this iterative process converges, it converges to a solution of the original equations with a consistent mass.

Nothing is known about the uniqueness of m_0: There is *a priori* no reason why the consistency condition could not be satisfied by an entirely different m_0 and thus different $L(E)$ and $L^{\times}(E)$. The question of uniqueness is obviously of physical interest. Computations have thus far shown no indication of a second solution, but the general question is still open. Fixed-point methods[11] seem out of the question because of the complicated structure of the model.

D. Details of Computation

Numerical integration was done with a ten-point Gaussian quadrature, after transforming the region of integration from $(1, \infty)$ to $(-1, 1)$. The matrices L and $L^{\times}$ were calculated at a fixed set of points $-\infty<E_i<1$, and other values obtained by interpolation. Nearly half the points were chosen in the region $(-1, 1)$ about the nucleon pole; the rest extended to large negative E, where the T matrix is approximately the potential term. For the reasons explained above, the matrix $L_{-\omega,\omega'}(E)$ was calculated at $E=E_i-\omega$, rather than $E=E_i$.

The iterative procedure described above was used to find a solution of the equations. For the weakest coupling, $g_0^2\approx 1$, the methods of Appendix B were unnecessary, and convergence was obtained in five iterations. For the strongest coupling tried, $g_0^2=50$, $q=0.05$ was used in the interpolated iteration, and 15 iterations were needed. The renormalized g^2 was obtained from the residue of the $E=0$ pole in $T(E)$, extrapolated onto the energy shell. The bound-state energy was found from the zero of $D^{\times}(E)$.

The computations were performed on an IBM 360/65 computer. Each iteration took slightly over 1 min to perform.

[11] For a discussion see H. McDaniel and R. W. Warnock, Phys. Rev. **180**, 1433 (1969).

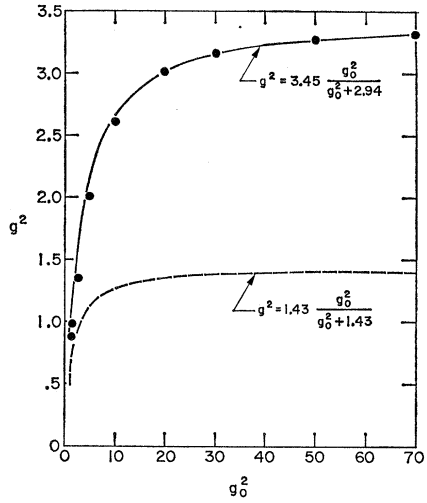

FIG. 4. Renormalized coupling constant g^2 versus unrenormalized coupling constant g_0^2. The dashed curve is obtained from the sum of bubbles. Solid curve is a least-squares fit to the large-g_0^2 points.

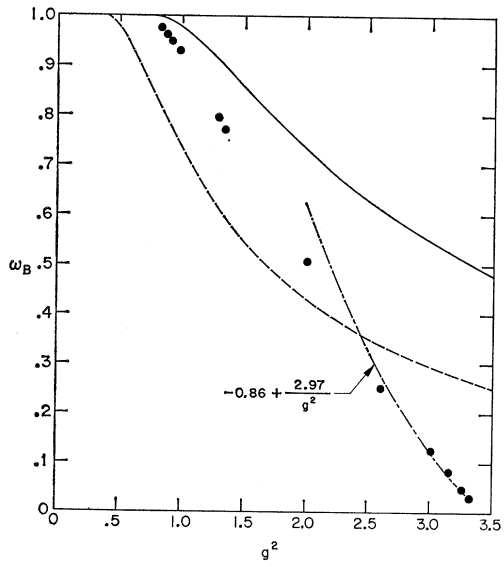

FIG. 5. Isobar bound-state energy ω_B (in units of the pion mass) versus the renormalized coupling constant g^2. Solid line is the one-meson approximation result. Dashed line is obtained from a variant of strong-coupling theory (see text). Dot-dashed line is a least-squares fit to the four largest-g^2 points.

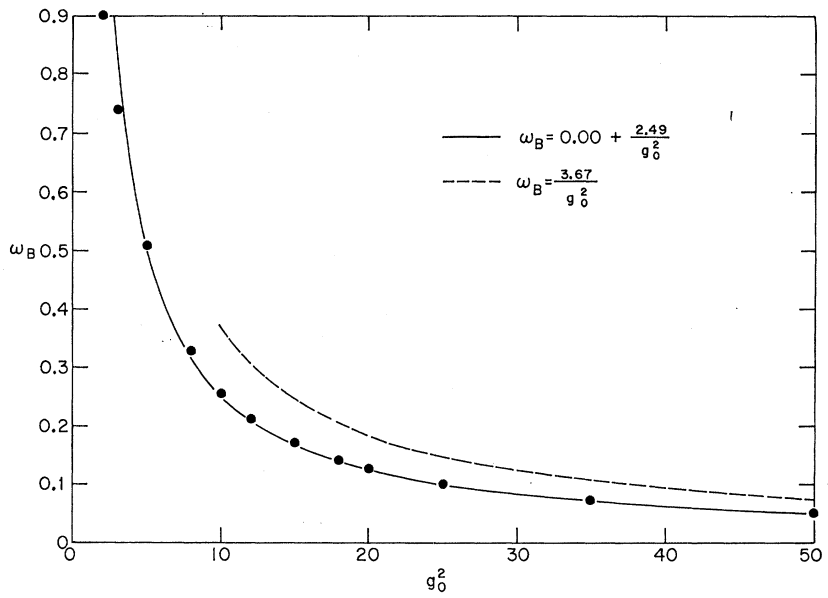

FIG. 6. Isobar bound-state energy ω_B versus the unrenormalized coupling constant g_0^2. Dashed line is the strong-coupling limit and solid line is a least-squares fit to the large-g_0^2 points.

V. RESULTS AND DISCUSSION

As mentioned above, for numerical calculation the cutoff function was taken such that $f^2(k)=2\pi^2/(\alpha^2k^2+1)$, with $\alpha=\frac{1}{5}$. The results of varying α are being accumulated and will be reported in a second paper.

A. Renormalized Coupling Constant

Figure 4 is a graph of the renormalized coupling constant g^2 plotted against the unrenormalized coupling constant g_0^2.[12] The dashed curve is the result obtained for the sum of bubbles [i.e., from $V(E)$ alone] given by $g^2=1.43g_0^2/(g_0^2+1.43)$. The solid curve is a least-squares fit to the large-g_0^2 points, $g^2=3.45g_0^2/(g_0^2+2.94)$.

The behavior $g^2\to$ const as $g_0^2\to\infty$ displayed by our model is similar to the Lee model[13] and in contrast to the behavior[7] $g^2\to\frac{1}{4}g_0^2$ as $g_0^2\to\infty$ of the charged scalar theory. If the limit $g^2\to\infty$ were studied in our model—for example, by using on-shell dispersion relations—we believe that ghosts would appear as they do in the Lee model.[13]

B. N^{++} Bound-State Energy

Figure 5 shows the isobar bound-state energy ω_B plotted as a function of g^2. The solid line is obtained from the one-meson approximation.[14] The deviation of our points below the solid line makes the effect of inelastic states quite evident.

The dashed line is obtained by extending Goebel's strong-coupling model.[7] It is included to illustrate how strong the inelastic effects in our model are. The extension involves using Goebel's result from his strong-coupling calculation of $\omega_B(g^2)$ at small g^2. We remind the reader that Goebel's result is obtained by applying the Chew-Low equation to charged scalar theory and assuming that the elastic and inelastic cross sections are equal at all energies in both the π^-p and π^+p channels. The equality of the elastic and inelastic cross sections stems from the fact that $\pi^-p\to\pi^-p$ and $\pi^-p\to\pi^+N^-$ become identical in the strong-coupling limit, as do $\pi^+p\to\pi^+p$ and $\pi^+p\to\pi^-N^{+++}$. On the other hand, the production amplitudes vanish as $1/g^2$, so, for example, $\pi^-p\to\pi^-\pi^+N$ does not contribute to π^-p elastic scattering.

Figure 5 shows that the inelastic states in our model more than make up for the lack of charge-exchange effects. This is evident from a comparison of our data with the two curves in the figure. These curves show the effect of increasing g^2 in two simple models, one without any inelastic effects and the other with inelastic effects proportional to the elastic effects.

A least-squares fit to our points at large g_0^2 gives $\omega_B=-0.86+2.97/g^2$. Extrapolation of this fit to ω_B less than zero requires g^2 to exceed the maximum value allowed by our model. We note that $\omega_B=0$ when $g^2=3.44$, which may be compared with $g_{\max}^2=3.45$ from Fig. 4.

Figure 6 displays ω_B as a function of g_0^2. The dashed line is the strong-coupling limit, $\omega_B=(8/\pi)(1+\alpha)^2/g_0^2$ (using $g^2\to\frac{1}{4}g_0^2$ as $g_0^2\to\infty$), and the solid line is a least-squares fit to our points for large g_0^2, $\omega_B=-0.00+2.48/g_0^2$.

Thus we have the result $\omega_B\to 0$ (within our numerical precision) as $g_0^2\to\infty$. In contrast to charged scalar

[12] The points plotted on the graphs of this section are our computed results. Accurate error analysis of numerical computations such as ours is very difficult, but a maximum error of 1% in our numbers seems reasonable.

[13] G. Källén, in *Lectures in Theoretical Physics* (W. A. Benjamin, Inc., New York, 1962), Vol. I.

[14] Our cutoff is used in calculating this line. The result provides a rigorous upper bound for ω_B.

theory, our model lacks a compelling argument as to why this should happen. In charged scalar theory the argument that $\omega_B \to 0$ as g^2 (the renormalized coupling constant) $\to\infty$ runs roughly as follows. In $\pi^- p$ elastic scattering the neutron pole is given by g^2/ω and the crossed isobar pole by $-\tilde{g}^2/(\omega+\Delta)$. Since these are known to be the only two poles as $g^2\to\infty$, at least we must have $\tilde{g}^2 \to g^2+O(1)$, $\Delta \to O(1/g^2)$ to ensure that unitarity is satisfied.

In our model this argument fails since g^2 remains finite. In the Lee model g^2 also remains finite in the limit $g_0^2\to\infty$ and the V-θ bound-state pole nevertheless approaches the N pole.[15] In that case the bound state and the N pole do not cancel; however, as discussed below, this cancellation does occur in our model.

C. Renormalized Mass

Figure 7 shows that m_0 grows like g_0^2 in our model. This is in agreement with charged scalar theory. In the strong-coupling limit, charged scalar theory[6] gives $m_0=\pi g_0^2/8a$, where

$$\frac{1}{a}=\left(\frac{1}{2\pi}\right)^3\int d^3k\,\frac{1}{\alpha^2k^2+1}\,\frac{4\pi}{k^2+1}=\frac{1}{\alpha(1+\alpha)}$$

in our notation. This gives $m_0=(25\pi/48)g_0^2=1.64g_0^2$, compared with our model, which gives $m_0=5.6g_0^2$. This is consistent with our other results, which show the large binding effects of the inelastic states.

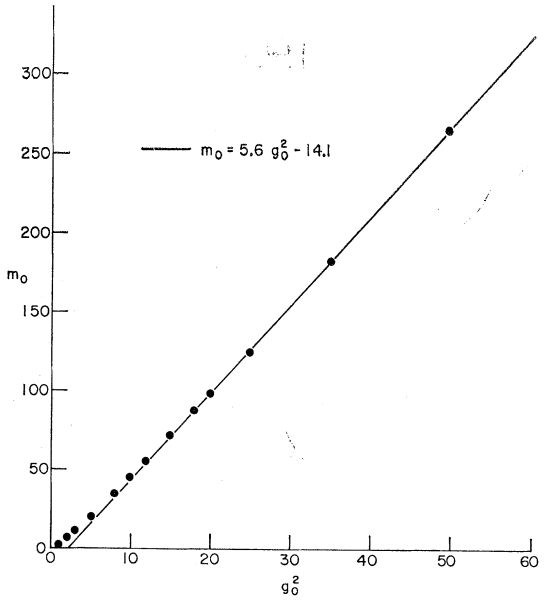

FIG. 7. Unrenormalized neutron mass m_0 versus g_0^2. Solid line is a least-squares fit to the large-g_0^2 points.

[15] M. T. Vaughn, R. Aaron, and R. D. Amado, Phys. Rev. **124**, 1258 (1961).

D. Fredholm Determinants

The Fredholm determinants for $\pi^- p$ and $\pi^+ p$ elastic scattering are defined by

$$D(E)=\det\{1-[V(E)+L(E)]G(E)\}$$

and

$$D^\times(E)=\det\{1-[V^\times(E)+L^\times(E)]G(E)\},$$

respectively. It is well known, or in any case simple to prove, that they are analytic functions in the complex E plane cut from 1 to ∞. Furthermore, in the region of elastic scattering, $1\leq E\leq 2$, the s matrix for $\pi^- p$ is given

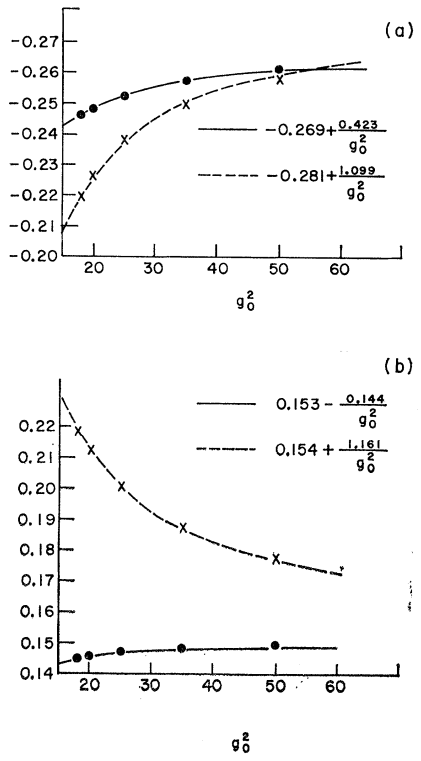

FIG. 8. (a) Dots and crosses are the values of D and $D^\times$, respectively, at $E=0.5$ pion mass. The lines are least-squares fits to the computed points. (b) The same as (a), for $D(-0.5)$ and $D^\times(-0.5)$.

by $S(E)=e^{2i\delta(E)}=D(E-)/D(E+)$, and similarly for $\pi^+ p$.

In Fig. 8, we have plotted D and $D^\times$ against g_0^2, for large g_0^2, at two representative E's. It is evident that D and $D^\times$ approach each other. This might be expected, since the masses of the two pole terms n and N^{++} become equal.

The line in Fig. 9 is the extrapolated value of D and $D^\times$ in the infinite-g_0^2 limit. The points and crosses are the computed values of D and $D^\times$, respectively, for $g_0^2=50$, the highest value of g_0^2 we have used.

From our results it follows that the N^{++}-p-π^+ coupling constant becomes equal to g^2 and that elastic $\pi^- p$ and $\pi^+ p$ scattering become identical in the infinite-

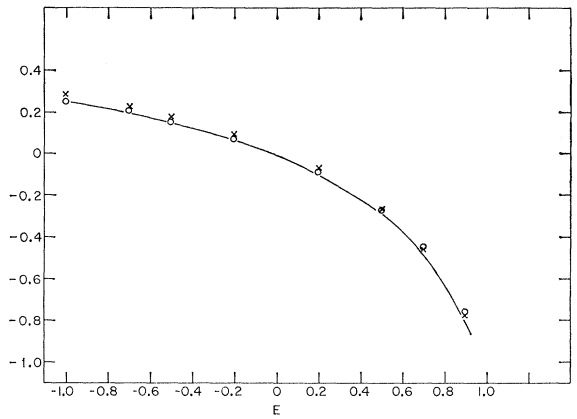

FIG. 9. Plot of $D(E)=D^{\times}(E)$ versus E (in units of the pion mass), obtained by extrapolating to infinite unrenormalized coupling constant g_0^2. The points and crosses are the values of $D(E)$ and $D^{\times}(E)$, respectively, for $g_0^2=50$.

g_0^2 limit. These results agree with the strong-coupling limit of charged scalar theory[7] in the sense that the two channels have identical scattering. It seems reasonable that the equality of D and $D^{\times}$ in our model implies the equality of $\pi^- p$ and $\pi^+ p$ elastic and inelastic scattering at all energies.

VI. CONCLUSIONS

We have found that an iterative scheme based on crossing and elastic unitarity, supplemented with the technical methods of Appendix B, gives convergent results over the entire range of g_0^2. This leads us to conclude that such methods would yield solutions for other more realistic models. The general prescription is to satisfy unitarity in each channel and use crossing to obtain the effective potential. What appears important to us is that in at least one case this program can be made to yield a solution.

When applied to relativistic scattering, this approach meets two difficulties. One is simply the increased number of variables and multidimensional unitarity integrals—this merely increases the computational requirements for the problem. The other is the fact that it does not seem possible to stay below elastic threshold in the calculations; if this is indeed the case, methods are needed for dealing numerically with singular integrals. While in principle neither difficulty makes obtaining a solution impossible, each weighs against the practicality of trying.

The method is of interest only if it can be argued that the omission of multiparticle unitarity is not a fatal defect. The correct behavior of the isobar in our model suggests that this is the case.

ACKNOWLEDGMENTS

One of the authors (M.H.R.) wishes to express his thanks to Dr. V. Barger for his hospitality at University of Wisconsin Conference on High-Energy Physics, where a preliminary version of this work was presented. He is also grateful to Dr. C. J. Goebel for interesting conversations related to this work.

APPENDIX A: NOTATION

In our notation the interaction Hamiltonian for the charged scalar model is

$$H_I=g_0\int\frac{d^3k\,f(k)}{2\omega(2\pi)^{3/2}}[\tau_+\mathfrak{A}_+(k)+\tau_-\mathfrak{A}_-(k)]+\text{H.c.},$$

where $\mathfrak{A}_\pm(k)$ destroys a $\pi^\pm$,

$$[\mathfrak{A}_\pm(k),\mathfrak{A}_\pm^\dagger(k')]=2\omega\delta^3(k'-k),$$

$$\tau_+=\begin{pmatrix}0&1\\0&0\end{pmatrix}=\tau_-^\dagger,\quad \omega=(k^2+1)^{1/2},$$

and H.c. means Hermitian conjugate. $f^2(k)=2\pi^2/(\alpha^2k^2+1)$, where $1/\alpha$ is the momentum cutoff. $\alpha=0$ corresponds to a point nucleon.

Our T matrix satisfies the unitarity condition

$$\mathrm{Im}T_{\omega\omega}^{-1}(\omega)=(1/4\pi)(\omega^2-1)^{1/2}.$$

APPENDIX B

This appendix presents two useful methods for transforming a divergent iterative process to a convergent one, or, alternatively, to improve an already convergent one. The methods involve only trivial extensions of known results, and closely follow Ref. 10. They are given in detail here simply because they seem to be unknown, or known only as rule-of-thumb procedures, to many physicists. Although the exposition assumes Fredholm equations, it is clear that it is applicable to iterative solutions for a wide class of problems. In the present case, the methods were applied without modification to three independent variables in two coupled equations with satisfactory results.

A. Interpolated Iteration

Assume an initial iterative process

$$y_{n+1}=F(y_n) \tag{B1}$$

to find a solution to $y=F(y)$. The estimates y_n and y_{n+1} can be interpolated to give an estimate

$$\tilde{y}_{n+1}=(1-q)y_n+qy_{n+1}=(1-q)y_n+qF(y_n). \tag{B2}$$

This yields what is called the interpolated iterative process.

It is claimed that for a proper choice of q this modification can make a divergent procedure convergent. To see this we need a method of measuring convergence.

Consider the iteration of a general nonlinear Fredholm

equation

$$y_{n+1}(x)=\int dt\, k(x,t;y_n(t))+f(x)=F(y_n(t)). \quad \text{(B3)}$$

If $y(x)$ is the exact solution,

$$y(x)-y_{n+1}(x)\approx\int dt\frac{\partial k}{\partial y}(x,t;y(t))[y(x)-y_n(x)]. \quad \text{(B4)}$$

We assume that $\partial k/\partial y$ has a complete set of eigenfunctions φ_i and eigenvalues λ_i. We then expand

$$y(t)-y_0(t)=\sum_i a_i\varphi_i(t), \quad \text{(B5)}$$

$$y(t)-y_1(t)=\sum_i a_i\lambda_i\varphi_i(t), \quad \text{(B6)}$$

$$\begin{aligned} y(t)-y_n(t)=\sum_i a_i\lambda_i{}^n\varphi_i(t)&\approx a_{\max}\lambda_{\max}{}^n\varphi_{\max}(t)\\ &\approx\lambda_{\max}[y(t)-y_{n-1}(t)], \end{aligned} \quad \text{(B7)}$$

where $\lambda_{\max}$ is the (assumed real) eigenvalue of maximum modulus. For $\lambda_{\max}$ one of a complex-conjugate pair [this is possible because the kernal of Eq. (4) is not symmetric], Eq. (7) is modified in an obvious way. Clearly, the iterative procedure coverages for $|\lambda_{\max}|<1$.

For the interpolated iteration scheme

$$\tilde{y}_{n+1}(x)=(1-q)\tilde{y}_n(x)+qF(\tilde{y}_n(x)), \quad \text{(B8)}$$

one has the new eigenvalues

$$\begin{aligned} \tilde{\lambda}_i&=1-q+q\lambda_i,\\ 1-\tilde{\lambda}_i&=q(1-\lambda_i). \end{aligned} \quad \text{(B9)}$$

Thus, the effect of interpolation is to bring the eigenvalues towards 1 as q goes to zero. For real $\lambda_{\max}$, the correct choice of sign for q will ensure $|\lambda_{\max}|<1$ for sufficiently small q.

Clearly the optimum choice of q is $(1-\lambda_{\max})^{-1}$; a smaller value will simply slow convergence. The usefulness of this method lies in the fact that $\lambda_{\max}$, which in all likelihood is quite inaccessible, need not be known—one simply seeks the largest $|q|<1$ that gives convergence. The reason that the largest value is preferable is given below.

B. Aitken's Extrapolation Formula

Given a convergent iterative procedure, such as that provided by interpolated iteration, it is possible to achieve much the same optimization as if $\lambda_{\max}$ were *a priori* known. We take (7) at $n-1$ and n to find

$$\lambda_{\max}\approx[y_{n+1}(t)-y_n(t)]/[y_n(t)-y_{n-1}(t)]=\lambda_n. \quad \text{(B10)}$$

We then have

$$y(t)\approx y_n(t)+[1/(1-\lambda_n)][y_{n+1}(t)-y_n(t)] \quad \text{(B11)}$$

as a better approximation than y_{n-1}, y_n, or y_{n+1}. To be valid, (7) must hold to a good approximation; the simplest way to verify this is to require $\lambda_n\approx\lambda_{n+1}$ to within some reasonable tolerance.

One way to regard this approach is as the Newton-Raphson method, but employing finite differences instead of an analytic derivative. The latter may well be too complicated to warrant its use, in spite of the improvement in convergence that it yields; this was the case in the present work.

It is necessary to use some care in employing the two methods in conjunction. A choice of q that is too small will slow convergence by bringing $\lambda_{\max}$ too near 1. Aitken's extrapolation will in large measure remedy this; however, with $\lambda_{\max}$ very near 1, Eq. (11) introduces very large corrections to y_n, and correspondingly large errors. This underscores the desirability of choosing q as large as possible.

C. Multiple Eigenvalues

When several eigenvalues of equal or nearly equal modulus are present, the above methods run into difficulty. For example, with two real eigenvalues $\lambda_1>1$ and $\lambda_2=1-\lambda_1$, it is clear that interpolated iteration with *any* $q\neq 0$ will have one transformed eigenvalue above 1, and hence will remain divergent. However, a choice of q sufficiently small will reduce the speed of divergence to manageable proportions, so that Aitken's method can be applied without large differences appearing between iterations.

Aitken's method itself has a straightforward modification for complex-conjugate eigenvalues, given in Ref. 10. This is equally applicable for two real eigenvalues, and should substantially speed convergence when both are important. However, two circumstances weigh against indiscriminate use of this modification. First, the method requires five iterations to obtain the extrapolation parameters, as opposed to three for the simple Aitken extrapolation. When, as in the present case, each iteration is time-consuming and complicated, this added cost may prove not worthwhile. Second, when one of the eigenvalues is of relatively minor importance (either because of a smaller modulus or because the difference between the approximate and exact solution happens to be orthogonal to its eigenfunction), this is reflected in significant uncertainties in the extrapolation parameters. The resulting extrapolation may well be no improvement over that from the simpler method.